Nucleophilic behaviour of the neutral complexes [M(C^P)-(S₂CNMe₂)] [M = Pd, Pt; C^P = CH₂C₆H₄P(C₆H₄Me-*o*)₂-κ-*C*,*P*] towards Ag(I) and Au(I) compounds. Synthesis (M = Pd, Pt) and molecular structures (M = Pt) of polynuclear complexes containing M–Ag and M–S bonds

J. Forniés,[a] A. Martín,[b] R. Navarro,[a] V. Sicilia,[a] P. Villarroya[a] and A. G. Orpen[b]

[a] *Departamento de Química Inorgánica, Instituto de Ciencia de Materiales de Aragón, Universidad de Zaragoza-C.S.I.C., 50009 Zaragoza, Spain*
[b] *School of Chemistry, University of Bristol, Bristol, UK BS8 ITS*

The reactions between [M{CH₂C₆H₄P(C₆H₄Me-*o*)₂}(S₂CNMe₂)] (M = Pt **A**, Pd **B**) and [M′(OClO₃)(PPh₃)] (M′ = Ag, Au) in 1:1 ratio yielded [M{CH₂C₆H₄P(C₆H₄Me-*o*)₂}(S₂CNMe₂)M′(PPh₃)]ClO₄ (M′ = Ag, M = Pt **1**, Pd **2**; M′ = Au, M = Pt **3**, Pd **4**). The molecular structure of **1** indicates that the Ag and Pt atoms are bridged by one S atom of the S₂CNMe₂ ligand and show a weak interaction between them [Pt–Ag 2.875 (1) Å]. Complexes **A** and **B** also react with AgClO₄ in 1:1 molar ratio to give [M₂{CH₂C₆H₄P(C₆H₄Me-*o*)₂}₂(S₂CNMe₂)₂Ag{Ag(OClO₃)}]ClO₄ (M = Pt **5**, Pd **6**). The X-ray study of **5** revealed that this compound crystallized as a mixture of [Pt₂{CH₂C₆H₄P(C₆H₄Me-*o*)₂}₂(S₂CNMe₂)₂Ag{Ag(OClO₃)}]ClO₄ and [Pt₂{CH₂C₆H₄P(C₆H₄Me-*o*)₂}₂(S₂CNMe₂)₂{Ag(OH₂)}{Ag(OClO₃)}]ClO₄ in 1:1 molar ratio. In the two different cations only one Ag atom is bonded to Pt, with the Pt–Ag lengths being 2.671 (3) Å for [Pt₂{CH₂C₆H₄P(C₆H₄Me-*o*)₂}₂(S₂CNMe₂)₂Ag{Ag(OClO₃)}]⁺ and 2.752(3) Å for [Pt₂{CH₂C₆H₄P(C₆H₄Me-*o*)₂}₂(S₂CNMe₂)₂{Ag(OH₂)}{Ag(OClO₃)}]⁺, both in the range found in other compounds with Pt–Ag bonds. Compounds **5** and **6** react with PPh₃ in 1:2 molar ratio to give compounds **1** and **2** respectively.

Introduction

Anionic organometallic complexes of Pt(II) with perhalophenyl ligands are known to react with a variety of Ag⁺ derivatives to afford heteronuclear compounds displaying donor–acceptor Pt^{II}⟶Ag^{I} bonds,[1] in many cases unsupported by any covalent bridging ligand. In contrast, neutral perhalophenyl derivatives do not yield similar Pt–Ag complexes. As far as we know, only a small number of Pt–Ag complexes involving neutral Pt(II) fragments have been described,[2–8] and structurally characterized.[4–8] In the latter complexes there are ligands bridging between the Pt and Ag atoms.
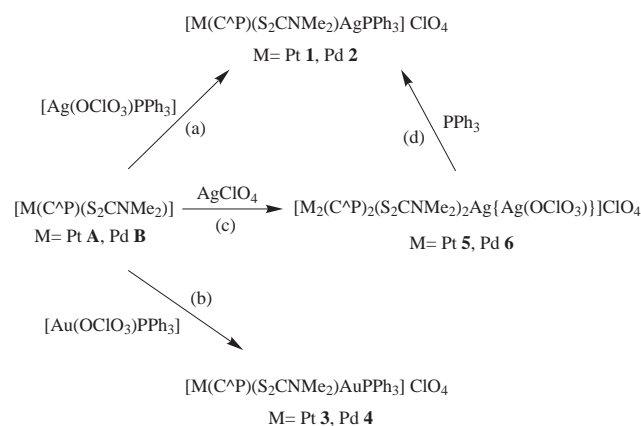
Recently we have described the synthesis of the neutral complexes [M{CH₂C₆H₄P(C₆H₄Me-*o*)₂}(S₂CZ)] (M = Pt, Pd; Z = NMe₂, OEt)[9] and we have demonstrated their ability to form donor–acceptor M–Hg bonds, unsupported by any covalent bridging ligands, when they are reacted with HgX₂ (X = Br, I).[9b] This indicates that in these complexes the metal centre, M, must have an excess of available electron density to act as a Lewis base toward suitable Lewis acids.

For this reason we have decided to explore the reactivity of the compounds [M{CH₂C₆H₄P(C₆H₄Me-*o*)₂}(S₂CZ)] (M = Pt, Pd; Z = NMe₂, OEt) towards other Lewis acids such as [M′(OClO₃)(PPh₃)] (M′ = Ag, Au) and AgClO₄ in order to prepare heteropolynuclear complexes, to study their structures and to establish the influence of the sulfur containing ligands in the formation of the Pt–M′ bonds. While [M{CH₂C₆H₄P(C₆H₄Me-*o*)₂}(S₂COEt)] (M = Pt, Pd) react with AgClO₄ and [M′(OClO₃)(PPh₃)] (M′ = Ag, Au) with decomposition, [M{CH₂C₆H₄P(C₆H₄Me-*o*)₂}(S₂CNMe₂)] (M = Pt **A**, Pd **B**) afford new complexes which are the subject of this paper.

Results and discussion

Reactivity of complexes [M{CH₂C₆H₄P(C₆H₄Me-*o*)₂}-(S₂CNMe₂)] (M = Pt A, Pd B) with [Ag(OClO₃)(PPh₃)], [Au(OClO₃)(PPh₃)] and AgClO₄

The reactions carried out are collected in Scheme 1.

[M(C^P)(S₂CNMe₂)AgPPh₃] ClO₄
M= Pt **1**, Pd **2**

[Ag(OClO₃)PPh₃]
(a)

PPh₃
(d)

[M(C^P)(S₂CNMe₂)]
M= Pt **A**, Pd **B**

AgClO₄
(c)

[M₂(C^P)₂(S₂CNMe₂)₂Ag{Ag(OClO₃)}]ClO₄
M= Pt **5**, Pd **6**

[Au(OClO₃)PPh₃]
(b)

[M(C^P)(S₂CNMe₂)AuPPh₃] ClO₄
M= Pt **3**, Pd **4**

Scheme 1

As is to be expected, the reactions of [M{CH₂C₆H₄P(C₆H₄-Me-*o*)₂}(S₂CNMe₂)] (M = Pt **A**, Pd **B**) with [Ag(OClO₃)(PPh₃)] in 1:1 molar ratio in the dark gave [M{CH₂C₆H₄P(C₆H₄-Me-*o*)₂}(S₂CNMe₂)Ag(PPh₃)]ClO₄ (M = Pt **1**, Pd **2**), which could be isolated as stable solids in good yield [Scheme 1(a)].

Table 1 Crystal data and structure refinement for $1\cdot1.5CHCl_3$ and $5\cdot0.5H_2O\cdot0.5CHCl_3\cdot0.125C_6H_{14}$ [a]

	$1\cdot1.5CHCl_3$	$5\cdot0.5H_2O\cdot0.5CHCl_3\cdot0.125C_6H_{14}$
Empirical formula	$C_{42}H_{41}AgClNO_4P_2PtS_2\cdot1.5CHCl_3$	$C_{48}H_{52}Ag_2Cl_2N_2O_8P_2Pt_2S_4\cdot0.5H_2O\cdot0.5CHCl_3\cdot0.125C_6H_{14}$
M	1267.28	1731.38
$a/Å$	13.312(4)	13.1745(25)
$b/Å$	14.145(5)	14.3883(25)
$c/Å$	14.793(5)	17.6371(27)
$a/°$	112.19(3)	84.071(12)
$\beta/°$	99.97(3)	85.845(12)
$\gamma/°$	101.18(3)	83.872(12)
$U/Å^3$	2435.3(14)	3300.0(10)
$D_c/Mg\,m^{-3}$	1.728	1.742
μ/mm^{-1}	3.765	5.173
$F(000)$	1246	1672
Crystal size/mm	$0.50 \times 0.30 \times 0.30$	$0.55 \times 0.45 \times 0.35$
θ range for data collection/°	1.54–25.00	1.56–23.27
Index ranges	$0 \leqslant h \leqslant 15, -16 \leqslant k \leqslant 16, -17 \leqslant l \leqslant 17$	$-14 \leqslant h \leqslant 10, -15 \leqslant k \leqslant 15, -19 \leqslant l \leqslant 19$
Reflections collected	9042	14032
Independent reflections (R_{int})	8584 (0.0220)	9203 (0.0291)
Data, restraints, parameters	8583, 6, 632	9200, 36, 707
Goodness-of-fit [b] on F^2	1.239	1.837
Final R indices [b] $[I > 2\sigma(I)]$: $R1$, $wR2$	0.0451, 0.1263	0.0512, 0.1517
R indices (all data): [b] $R1$, $wR2$	0.0568, 0.1340	0.0626, 0.1635
Largest difference peak, hole/e Å^{-3}	2.702, −1.972	1.354, −0.901
$g(w)$ [b]	0.0800	0.0600

[a] Details in common: triclinic, space group $P\bar{1}$, $T = 293(2)$ K, $Z = 2$, $\lambda = 0.71073$ Å; full matrix least-squares refinement on F^2. [b] $R1 = \Sigma||F_o| - |F_c||/\Sigma|F_o|$; $wR2 = \{\Sigma[w(F_o^2 - F_c^2)^2/\Sigma[w(F_o^2)^2]\}^{\frac{1}{2}}$; $w = [\sigma_c^2(F_o^2) + (gP)^2]^{-1}$, where $P = [Max(F_o^2, 0) + 2F_c^2]/3$; goodness of fit $= [w(F_o^2 - F_c^2)^2/(N - P)]^{\frac{1}{2}}$, where N, P are the numbers of observations and parameters, respectively.

**Table 2** Selected bond lengths (Å) and angles (°) for $[Pt(C^{\wedge}P)(S_2CNMe_2)Ag(PPh_3)]ClO_4$ **1**

Pt–C(1)	2.062(7)	Pt–Ag	2.875(1)
Pt–P(1)	2.240(2)	Ag–P(2)	2.383(2)
Pt–S(1)	2.369(2)	Ag–S(1)	2.594(2)
Pt–S(2)	2.405(2)		
C(1)–Pt–P(1)	85.0(2)	C(1)–Pt–S(1)	93.4(2)
P(1)–Pt–S(2)	107.7(1)	S(1)–Pt–S(2)	74.1(1)
Pt–S(1)–Ag	70.6(1)	S(1)–Ag–P(2)	165.0(1)
P(2)–Ag–Pt	131.5(1)	S(1)–Ag–Pt	51.0(1)

The gold(I) derivatives $[M\{CH_2C_6H_4P(C_6H_4Me-o)_2\}(S_2CNMe_2)Au(PPh_3)]ClO_4$ (M = Pt **3**, Pd **4**) were obtained by reaction of complexes $[M\{CH_2C_6H_4P(C_6H_4Me-o)_2\}(S_2CNMe_2)]$ (M = Pt **A**, Pd **B**) with $[Au(OClO_3)(PPh_3)]$ in 1 : 1 molar ratio [Scheme 1(b)]. The $[Au(OClO_3)(PPh_3)]$ species was generated *in situ* from $[AuCl(PPh_3)]$ and $AgClO_4$.

The structure of $[Pt\{CH_2C_6H_4P(C_6H_4Me-o)_2\}(S_2CNMe_2)Ag(PPh_3)]ClO_4$ **1** was established by a single crystal X-ray study. The structure of the cation is shown in Fig. 1. General crystallographic information is collected in Table 1. Selected bond distances and angles are given in Table 2.

As can be seen, the Pt atom displays a distorted square-pyramidal environment with the Pt, the C and P atoms of the $C^{\wedge}P$ group and both S atoms of the S_2CNMe_2 located in the basal plane and the Ag atom of the $[Ag(PPh_3)]^+$ fragment in the apical position. The angle between the Pt–Ag vector and the perpendicular to the basal plane [Pt, P(1), C(1), S(1), S(2)] is 29.5°. [10]

Distances and angles around the Pt center in the basal plane are similar to those observed in the starting complex $[Pt\{CH_2C_6H_4P(C_6H_4Me-o)_2\}(S_2CNMe_2)]$ [9a] or in $[Pt\{CH_2C_6H_4P(C_6H_4Me-o)_2\}(S_2CNMe_2)HgI(\mu-I)]_2$. [9b] As in these cases, the angles between *cis* ligands around the platinum center are rather different from 90° due to the small bite angles of both chelate ligands present in the complex. The metallocycle defined by the Pt, P(1), C(1), C(2), C(3) atoms is planar and coplanar with the C-bonded *o*-tolyl ring. [10] The other two *o*-tolyl rings are also planar, and they are oriented forming a dihedral
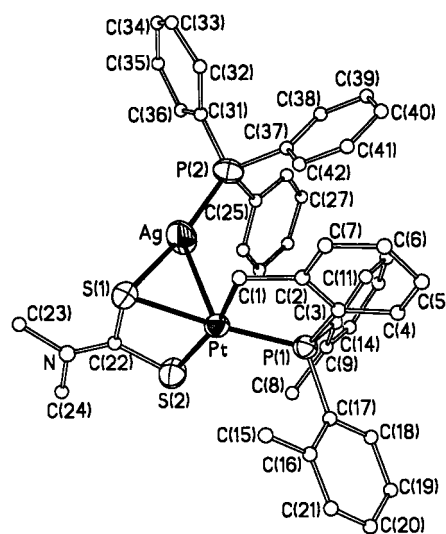
Fig. 1 Molecular structure and atomic numbering scheme of the cation in **1**.

angle of 63.59° [C(8)–C(14)] and 89.79° [C(15)–C(21)] respectively with the metallocyle plane [Pt, P(1), C(1), C(2), C(3)].

The platinum and silver fragments, $[Pt\{CH_2C_6H_4P(C_6H_4Me-o)_2\}(S_2CNMe_2)]$ and $[Ag(PPh_3)]$, share one sulfur atom of the dithiocarbamate group, leading to a very acute Pt–S(1)–Ag angle [70.6 (1)°] probably as a consequence of the interaction between the metal centers. The Ag atom is also coordinated by the PPh_3 ligand and more weakly by the Pt atom [Pt–Ag 2.875(1) Å]. The coordination environment and the angles around the Ag atom in **1** are similar to those in $[(PPh_3)(C_6Cl_5)ClPt(\mu-Cl)Ag(PPh_3)]$ [11] and $NBu_4[PtAgCl_2(C_6Cl_5)_2(PPh_3)]$ [12] in which the Pt and Ag centers are bridged by a Cl atom. The Ag–P [11–13] and Ag–S [5,8] bond distances, 2.383(2) and 2.594(2) Å respectively, are in the range found for other Pt–Ag complexes containing these kind of ligands.

The Pt–Ag distance [2.875(1) Å] is shorter than that corresponding to the sum of the van der Waals radii [14] for Pt and Ag and is in the range found in other complexes which exhibit

Table 3 $^{31}P\{^1H\}$ NMR data for complexes **1**–**6** [a]

	C^P		PPh₃	
Complex	$\delta(^{31}P)$	J_{PtP}/Hz	$\delta(^{31}P)$	J_{AgP}/Hz
[Pt(C^P)(S₂CNMe₂)] **A**	24.70 (s)	3969.4		
[Pd(C^P)(S₂CNMe₂)] **B**	35.58 (s)			
[Pt(C^P)(S₂CNMe₂)Ag(PPh₃)]ClO₄ **1** [b]	25.20 (s)	4011.4	9.1 (d)	
[Pd(C^P)(S₂CNMe₂)Ag(PPh₃)]ClO₄ **2** [c]	37.07 (s)		13.46 (2d)	^{109}Ag–P 714.36
				^{107}Ag–P 618.78
[Pt(C^P)(S₂CNMe₂)Au(PPh₃)]ClO₄ **3**	24.52 (s)	4156.8	32.83 (s)	
[Pd(C^P)(S₂CNMe₂)Au(PPh₃)]ClO₄ **4**	35.54 (s)		33.49 (s)	
[Pt₂(C^P)₂(S₂CNMe₂)₂Ag{Ag(OClO₃)}]ClO₄ **5**	24.93 (s)	3911.8		
[Pd₂(C^P)₂(S₂CNMe₂)₂Ag{Ag(OClO₃)}]ClO₄ **6** [c]	41.07 (s)			

[a] C^P = CH₂C₆H₄P(C₆H₄Me-o)₂; spectra recorded in CDCl₃ at room temperature unless otherwise stated; s = singlet. [b] T = 193 K, CD₂Cl₂. [c] T = 218 K, CDCl₃.

Table 4 ^1H NMR data for complexes **1**–**6** [a]

	C^P and PPh₃			
Complex	$\delta(CH_3)$	$\delta(CH_2)$ (J/Hz)	δ (aromatic)	$\delta(^-S_2CNMe_2)$
[Pt(C^P)(S₂CNMe₂)] **A**	2.42 (s)	3.38 (s, 1H, $^2J_{PtH}$ = 85.7)	6.9–7.3	3.23 (s)
	2.78 (s)	3.44 (s, 1H, $^2J_{PtH}$ = 94.3)		3.24 (s)
[Pd(C^P)(S₂CNMe₂)] **B**	2.44 (s)	3.38 (s, 2H)	6.7–7.4	3.29 (s)
	2.74 (s)			3.34 (s)
[Pt(C^P)(S₂CNMe₂)Ag(PPh₃)]ClO₄ **1**	2.30 (s)	3.31 (2H, $^2J_{PtH}$ = 89)	6.8–7.5	3.36 (s)
	2.64 (s)			3.39 (s)
[Pd(C^P)(S₂CNMe₂)Ag(PPh₃)]ClO₄ **2**	2.32 (s)	3.33 (s, 2H)	6.8–7.6	3.44 (s)
	2.63 (s)			3.52 (s)
[Pt(C^P)(S₂CNMe₂)Au(PPh₃)]ClO₄ **3**	2.31 (s)	—[c]	6.8–7.7	3.45 (s)
	2.62 (s)			3.49 (s)
[Pd(C^P)(S₂CNMe₂)Au(PPh₃)]ClO₄ **4**	2.39 (s)	2.91 (s, 1H)	6.7–7.7	3.27 (s)
	2.69 (s)	3.16 (s, 1H)		3.31 (s)
[Pt₂(C^P)₂(S₂CNMe₂)₂Ag{Ag(OClO₃)}]ClO₄ **5**	2.28 (s)	3.08 (s, 1H)	6.7–7.7	3.34 (s)
	2.63 (s)	3.21 (s, 1H)		3.40 (s)
[Pd₂(C^P)₂(S₂CNMe₂)₂Ag{Ag(OClO₃)}]ClO₄ **6** [b]	2.12 (s)	3.08 (d, 1H, $^2J_{HH}$ = 11.13)	6.5–7.7	3.49 (s)
	2.65 (s)	3.37 (d, 1H)		3.54 (s)

[a] C^P = CH₂C₆H₄P(C₆H₄Me-o)₂; spectra recorded in CDCl₃ at room temperature unless otherwise stated; s = singlet, d = doublet. [b] 218 K. [c] CH signal obscured by Me₂NCS₂ signal.

Pt–Ag bonds. As example can be mentioned the compounds [Pt₃(S₂CNPr^{i}₂)₆Ag₂]BF₄[4] and [Pt₃(S₂CNBu^{n}₂)₆Ag₂]ClO₄[4] in which the Pt–Ag distances range from 3.061 to 2.825 Å and the interaction between both metal centers is indicated by the coupling of the nuclear spins observed in their ^{195}Pt NMR spectra. Unfortunately, our complexes are not soluble enough to measure the ^{195}Pt NMR spectra.

These compounds seem to retain their structure in solution, because their mass spectra (FAB⁺) show in all cases the molecular peak for the corresponding cation [M{CH₂C₆H₄P(C₆H₄Me-o)₂}(S₂CNMe₂)M′(PPh₃)]⁺ [988 (**1**), 900 (**2**), 1077 (**3**), 988 (**4**)].

The ^{31}P NMR spectra of **1** and **2** were measured at low temperature but this was not necessary for complexes **3** and **4**. According to their structure, compounds **1**–**4** show two signals due to the C^P and the PPh₃ groups (Table 3). The C^P give a singlet, which appears flanked by the corresponding ^{195}Pt satellites for complexes **1** and **3** [J_{PtP} = 4011.4 Hz (**1**), 4156.8 Hz (**3**)]. The signal due to M′PPh₃ appears as a singlet when M′ = Au (complexes **3** and **4**) or as two doublets when M′ = Ag (complexes **1** and **2**), because of the presence of two isotopes, ^{107}Ag and ^{109}Ag, each having spin I = 1/2. For complex **2** the two Ag–P coupling constants could be calculated as 218 K, with $J_{^{107}AgP}$ and $J_{^{109}AgP}$ = 618.78 and 714.36 Hz respectively. Similar values for J_{AgP} have been observed in other complexes containing the fragment 'Ag(PPh₃)' in e.g. [PtMe₂(bpy){Ag-(PPh₃)}]BF₄.[2] For complex **1**, J_{AgP} could not be observed, even when the ^{31}P NMR spectrum was measured at 193 K in CD₂Cl₂. The ^1H NMR spectra of compounds **1**–**4** also show the signals

due to the C^P and the PPh₃ groups in agreement with their structure (Table 4).

Complexes **1**–**4** show similar IR and NMR spectra and, on these bases, similar structures can be proposed. However, since it is well known that the Pd centres exhibit a lower tendency to involve in Pd→M bonds,[9b,15] it is possible that in complexes **2** and **4** the Pd and M′ fragments are only joined by the sulfur centers.

Complexes [M{CH₂C₆H₄P(C₆H₄Me-o)₂}(S₂CNMe₂)] (M = Pt **A**, Pd **B**) react also with AgClO₄ in 1:1 molar ratio in the dark to yield the heteronuclear complexes of stoichiometry [M₂{CH₂C₆H₄P(C₆H₄Me-o)₂}₂(S₂CNMe₂)₂Ag₂(ClO₄)₂] (M = Pt **5**, Pd **6**) according to Scheme 1(c). Compounds **5** and **6** are air-stable and can be stored in the dark for extended periods.

The IR spectra of **5** and **6** show in both cases absorptions due to the C^P and the S₂CNMe₂[16] ligands together with the corresponding ones to the ClO₄⁻ anion.[17] However, no absorptions assignable to the O₃ClO⁻ ligand can be observed.

The X-ray study of **5** [Fig. 2(a), (b)] revealed that, in the solid, only one ClO₄⁻ group is ionic whereas the other is bonded to one of the silver atoms, and also, that in 50% of the molecules, the second silver atom is bonded to one molecule of water [Fig. 2(b)]. This indicates that the crystallized compound is a mixture of [Pt₂{CH₂C₆H₄P(C₆H₄Me-o)₂}₂(S₂CNMe₂)₂-Ag{Ag(OClO₃)}]ClO₄ and [Pt₂{CH₂C₆H₄(C₆H₄Me-o)₂}₂(S₂CN-Me₂)₂{Ag(OH₂)}{Ag(OClO₃)}]ClO₄ in 1:1 molar ratio. However, it should be noted that the IR spectra of **5** and **6** show that no water is present in the non-crystalline solids. Also, the
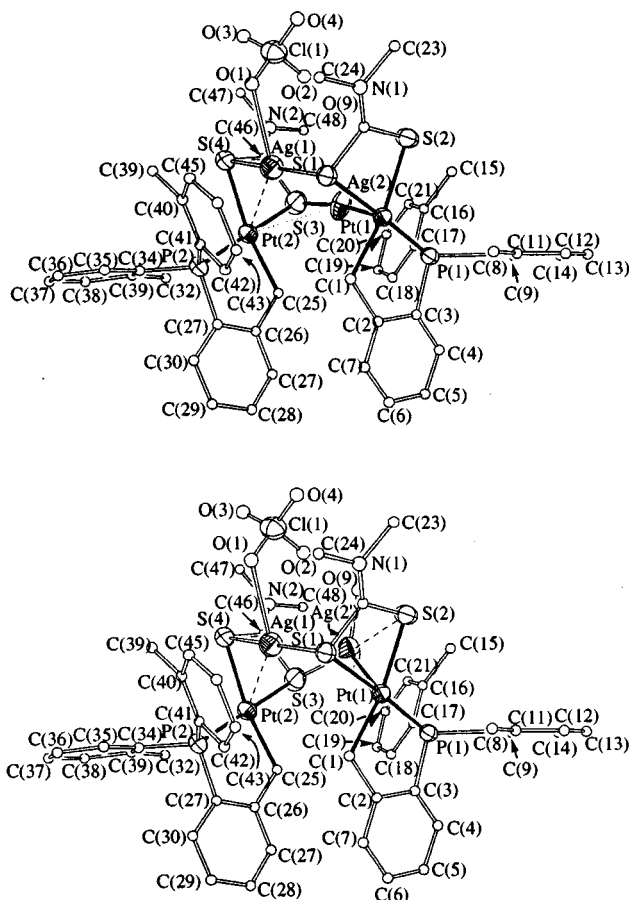
Fig. 2 Molecular structures and atomic numbering schemes of two views of the cation in **5**.

Table 5 Selected bond lengths (Å) and angles (°) for complex **5**

Pt(1)–C(1)	2.056(11)	Pt(2)–C(25)	2.071(12)
Pt(1)–P(1)	2.235(3)	Pt(2)–P(2)	2.228(3)
Pt(1)–S(1)	2.355(3)	Pt(2)–S(3)	2.369(3)
Pt(1)–S(2)	2.408(3)	Pt(2)–S(4)	2.409(3)
Pt(1)–Ag(2)	2.671(3)	Pt(2)–Ag(1)	2.907(1)
Pt(2)–Ag(2)	2.998(3)		
Ag(2)–S(3)	2.300(5)	Pt(1)–Ag(2′)	2.752(3)
Ag(1)–S(1)	2.485(3)	Ag(2′)–S(3)	2.694(5)
Ag(1)–O(1)	2.564(11)	Ag(2′)–O(9)	2.231(29)
Ag(1)–S(4)	2.660(3)	Ag(2′)–S(2)	2.941(5)
Ag(1)–Ag(2)	2.905(3)	Ag(1)–Ag(2′)	2.856(3)
C(1)–Pt(1)–P(1)	85.1(3)	S(1)–Ag(1)–O(1)	95.6(3)
C(1)–Pt(1)–S(1)	92.4(3)	O(1)–Ag(1)–S(4)	86.4(3)
P(1)–Pt(1)–S(2)	108.1(1)	S(1)–Ag(1)–S(4)	174.6(1)
S(1)–Pt(1)–S(2)	74.5(1)	S(3)–Ag(2)–Pt(1)	167.1(2)
C(25)–Pt(2)–P(2)	85.5(4)		
C(25)–Pt(2)–S(3)	93.4(4)	O(9)–Ag(2′)–Pt(1)	136.9(7)
P(2)–Pt(2)–S(4)	106.7(1)	S(3)–Ag(2′)–Pt(1)	130.2(2)
S(3)–Pt(2)–S(4)	74.4(1)	O(9)–Ag(2′)–S(3)	92.9(7)

$CNMe_2$) sub-units are in the range usually found for related compounds.[9,18–21] The dihedral angle between the square planes is 23.2°.[10]

The two silver atoms present in the cation show also different environments. Atom Ag(2) is bonded to Pt(1) [Pt(1)–Ag(2) 2.671(3) Å] and to one S [S(3)] atom of the Pt(2) sub-unit [Ag(2)–S(3) 2.300(5) Å] showing essentially a linear coordination mode [Pt(1)–Ag(2)–S(3) 167.1 (2)°]. The Ag(2) atom is located at 2.998(3) Å from the Pt(2), however the angle formed by the Pt(2)–Ag(2) vector and the perpendicular to the Pt(2) coordination plane is 43.9°, indicating that there is no Pt(2)–Ag(2) bond.

Atom Ag(1) is bonded to one S atom of each Pt sub-unit, [Ag(1)–S(1) 2.485(3) and Ag(1)–S(4) 2.660(3) Å], with the S(1)–Ag(1)–S(4) angle being 174.6(1)°. Ag(1) is also bonded to one oxygen atom of a perchlorate group [Ag(1)–O(1) 2.564(11) Å] showing a T-shaped coordination geometry. The Ag(1)–O(1) distance is shorter than those observed in other complexes with ClO_4 coordinated in monodentate [$Ag_2(napy)_2$]-(ClO_4)$_2$ [Ag–O 2.62(2) Å], (napy = 1,8-naphthyridine),[22] chelate [AgL(ClO_4)] {L = 2,11-bis[(diphenylphosphino)methyl]benzo-[c]phenanthrene} [Ag–O 2.75(1) and 2.81(1) Å][23] or bridge [$Ag_2(\mu$-dpph)$_2(\mu$-ClO_4)$_2$] (dpph = 1,6-bis(diphenylphosphino)-hexane) [Ag–O 2.639(4) and 2.712(6) Å][24] fashion, indicating that the Ag(1)–O(1) bond is relatively strong. Atom Ag(1) is located 2.907(1) Å away from the Pt(2) centre and is not close to the perpendicular to the Pt(2) coordination plane [Pt, C(25), P(2), S(3), S(4)], the angle between them being 52.4°.[10] These features suggest that no bond exists between the metal centers.

As we have already mentioned, half of the cations have the stoichiometry [Pt_2{$CH_2C_6H_4P(C_6H_4Me-o)_2$}$_2(S_2CNMe_2)_2${Ag-(OH_2)}{Ag(OClO_3)}$]$^+$ and their molecular structure is represented in Fig. 2(b). The structural data for this cation are not too different from those for [Pt_2{$CH_2C_6H_4P(C_6H_4Me-o)_2$}$_2$-($S_2CNMe_2$)$_2$Ag{Ag(OClO_3)}$]$^+$ [Fig. 2(a)] except those concerning the Ag(2′) and Ag(2) environments.
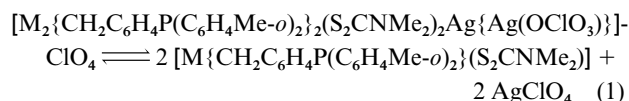
As is Ag(2), atom Ag(2′) is bonded to Pt(1) [Pt(1)–Ag(2′) 2.752(3) Å] and to one S atom from the Pt(2) sub-unit [Ag(2′)–S(3) 2.694(5) Å], but in contrast to Ag(2), atom Ag(2′) is also bonded to the oxygen atom of a water molecule [Ag(2′)–O(9) 2.23 (3) Å] showing a distorted triangular planar coordination environment instead of the linear arrangement displayed by Ag(2).

The Pt(1)–Ag(2′) distance [2.752(3) Å], is longer than Pt(1)–Ag(2) [2.671(3) Å], and this is in keeping with the following: (a) the angle between the perpendicular to the Pt(1) coordination plane and the Pt(1)–Ag(2′) vector (22.9°) is larger than the one formed with the Pt–Ag(2) vector (7.6°), indicating a poorer

FAB^+ spectra show the molecular peaks corresponding to [M_2{$CH_2C_6H_4P(C_6H_4Me-o)_2$}$_2(S_2CNMe_2)_2$Ag{Ag(OClO_3)}$]$^+$ cations (**5**, 1553; **6**, 1376). These facts lead us to formulate compounds **5** and **6** as [M_2{$CH_2C_6H_4P(C_6H_4Me-o)_2$}$_2$-($S_2CNMe_2$)$_2$Ag{Ag(OClO_3)}$]ClO_4 (M = Pt **5**, Pd **6**) and to consider that the coordination of water to one Ag atom of one half of the molecules took place during the crystallization process.

The molecular structure of the two different images of the cation observed in the crystal of **5** are shown in Fig. 2 together with the atomic numbering schemes. The only difference between them is the coordination mode of Ag(2) [Fig. 2(a)] or Ag(2′) [Fig. 2(b)]. General crystallographic information is collected in Table 1. Bond distances and angles are summarized in Table 5.

First, we will describe the structure of the cationic complex [Pt_2(C^P)$_2(S_2CNMe_2)_2$Ag{Ag(OClO_3)}$]$^+$ [C^P = $CH_2C_6H_4P$-($C_6H_4Me-o)_2$] [Fig. 2(a)]. As can be seen, the complex cation can be regarded as two Pt(C^P)(S_2CNMe_2) sub-units connected by two silver atoms. The platinum atoms show different coordination environments. Atom Pt(1) is located in a square pyramidal environment with Ag(2) sited in the apical position and the donor atoms of the C^P and S_2CNMe_2 chelating ligands in the basal plane. The Pt(1)–Ag(2) distance [2.671(3) Å] is at the low end of the range of distances found for other complexes with Pt–Ag bonds.[1] In addition, the angle between the Pt(1)–Ag(2) vector and the perpendicular to the Pt(1) coordination plane [Pt(1), C(1), P(1), S(1), S(2)] is only 7.6°.[10] Both facts indicate a Pt(1)–Ag(2) bond which is not supported by covalent bridging ligands.

On the other hand, atom P(2) shows a distorted square-planar environment formed by the donor atoms of the two chelate ligands bonded to it [C(25), P(2), S(3), S(4)]. Bond distances and angles around the platinum center in both Pt(C^P)(S_2-

overlap between the orbitals involved in the Pt(1)–Ag(2′) bond than the corresponding one to the Pt(1)–Ag(2) bond; (b) Ag(2′) is three-coordinate and because of this is less acidic than Ag(2), so that the Pt(1)–Ag(2′) bond should be weaker. The Ag(2′)–O(9) bond length [2.23(3) Å] is shorter than those observed in other silver–aquo complexes such as, *e.g.* [Ag$_2$(C$_9$H$_8$NO$_3$)$_2$-(H$_2$O)$_2$]·2H$_2$O [Ag–O 2.518(4) Å] [25a] and *cis*-[(NH$_3$)$_2$Pt(1-MeU)(1-MeC)Ag(OH$_2$)](NO$_3$)$_2$·Ag(NO$_3$)·2.5 H$_2$O (1 MeU = 1-methyluracilate, 1-MeC = 1-methylcytosine) [Ag–O 2.396(13) Å].[25b] Finally, although the Ag(2′) atom is located fairly close to the sulfur atoms of the Pt(1) sub-unit [Ag(2′)–S(2) 2.941(5) Å] any direct interaction, if present, is very weak.

It is noteworthy that in each view of the cation [Fig. 2(a) and (b)] the two Ag atoms are in close proximity [Ag(1)–Ag(2) 2.905(3), Ag(1)–Ag(2′) 2.856(3) Å]. These lengths are similar to the Ag–Ag distance in metallic silver (2.8894 Å) [26] and fall in the range of distances observed in complexes with silver–silver interactions.[27,28]

The ^{31}P NMR spectrum of **5** shows only one singlet with the corresponding ^{195}Pt satellites (see Table 3). Looking at the structure of **5** [Fig. 2(a)] this may be due to the fact that either **5** adopts a symmetrical molecular structure in solution or that dissociative processes take place on the NMR time scale [eqn. (1), M = Pd, Pt]. In the latter case, the observed signal will be

$$[M_2\{CH_2C_6H_4P(C_6H_4Me\text{-}o)_2\}_2(S_2CNMe_2)_2Ag\{Ag(OClO_3)\}]\text{-}$$
$$ClO_4 \rightleftharpoons 2\,[M\{CH_2C_6H_4P(C_6H_4Me\text{-}o)_2\}(S_2CNMe_2)] +$$
$$2\,AgClO_4 \quad (1)$$

the average of the corresponding signals for [Pt{CH$_2$C$_6$H$_4$P-(C$_6$H$_4$Me-*o*)$_2$}(S$_2$CNMe$_2$)] **A** and [Pt$_2${CH$_2$C$_6$H$_4$P(C$_6$H$_4$Me-*o*)$_2$}$_2$(S$_2$CNMe$_2$)$_2$Ag{Ag(OClO$_3$)}]ClO$_4$ **5**.

^{31}P NMR spectra of different mixtures of such compounds (**5** and **A**) were shown to give only one singlet at $\delta(^{31}$P) values between those corresponding to pure **5** (δ 24.93) and **A** (δ 24.7) and as the amount of **A** in the mixture was increased, the $\delta(^{31}$P) values move closer to the $\delta(^{31}$P) value for pure **A**. This observation indicates that the equilibrium represented by eqn. (1) is, in all likelihood, responsible for the observation of only one singlet in the ^{31}P NMR spectrum of **5**. In light of this equilibrium, AgClO$_4$ was added to a NMR sample of **5** with a view to obtaining its ^{31}P NMR signal, but a yellow solid precipitated in the NMR tube preventing a successful experiment. The signals observed in the ^{1}H NMR spectrum of **5** are in agreement with the equilibrium represented in eqn. (1) (Table 4).

The solution behaviour of compound **6** is similar to that observed for **5** (Tables 3 and 4).

As is to be expected, complexes **5** and **6** react with PPh$_3$ (in 1:2 molar ratio) in CH$_2$Cl$_2$ yielding the complexes [M-{CH$_2$C$_6$H$_4$P(C$_6$H$_4$Me-*o*)$_2$-*C*,*P*}(S$_2$CNMe$_2$)AgPPh$_3$]ClO$_4$ (M = Pt **1**, Pd **2**) [Scheme 1(d)].

Conclusion

[M{CH$_2$C$_6$H$_4$P(C$_6$H$_4$Me-*o*)$_2$}(S$_2$CNMe$_2$)] (M = Pt, Pd) act as Lewis bases towards [Ag(OClO$_3$)(PPh$_3$)], [Au(OClO$_3$)(PPh$_3$)] or AgClO$_4$ [M′] and the resulting polynuclear complexes contain not only Pt–M′ interactions but also S–M′ bonds. However, the way in which the platinum and [M′] fragments are connected is dependent on the [M′] moiety used. These results are in sharp contrast with the behaviour of [Pt{CH$_2$C$_6$H$_4$P(C$_6$H$_4$Me-*o*)$_2$}-(S$_2$CZ)] (Z = NMe$_2$, OEt) towards HgX$_2$ (X = Br, I) which results in the formation of the 1:1 adducts [{Pt{CH$_2$C$_6$-H$_4$P(C$_6$H$_4$Me-*o*)$_2$}(S$_2$CZ)HgX(μ-X)}$_2$] (Z = NMe$_2$, OEt; X = Br, I) in which the platinum fragments were connected to mercury through unsupported Pt→Hg donor–acceptor bonds.[9b]

Finally, it should be noted that given that palladium complexes are not so prone to form Pd–Ag bonds, the structure of the analogous Pd–Ag derivatives and the way in which the palladium substrates are connected to the silver fragment could

be rather different to that of the platinum complexes described above and should be established by X-ray diffraction study.[15]

Experimental

General procedures and materials

Elemental analyses were determined using a Perkin-Elmer 240-B microanalyzer. IR spectra were recorded on a Perkin-Elmer 599 spectrophotometer (Nujol mulls between polyethylene plates in the range 4000–200 cm^{-1}). NMR spectra were recorded on either a Varian XL-200 or a Varian Unity 300 NMR spectrometer using the standard references. [Pt{CH$_2$C$_6$-H$_4$P(C$_6$H$_4$Me-*o*)}(S$_2$CNMe$_2$)],[9a] [Pd{CH$_2$C$_6$H$_4$P(C$_6$H$_4$Me-*o*)$_2$}-(S$_2$CNMe$_2$)],[9b] [Ag(OClO$_3$)(PPh$_3$)] [13a] and [AuCl(PPh$_3$)] [29] were prepared by literature methods. All the reactions were carried out with exclusion of light.

CAUTION Perchlorate salts are potentially explosive. Only small amounts of material should be prepared and these should be handled with great caution.

[M{CH$_2$C$_6$H$_4$P(C$_6$H$_4$Me-*o*)$_2$-*C*,*P*}(S$_2$CNMe$_2$)AgPPh$_3$]ClO$_4$ (M = Pt 1, Pd 2)

M = Pt (1). *Method (a)*. [Ag(OClO$_3$)(PPh$_3$)] (0.1796 g, 0.38 mmol) was added to a solution of [Pt{CH$_2$C$_6$H$_4$P(C$_6$H$_4$Me-*o*)$_2$-*C*,*P*}(S$_2$CNMe$_2$)] **A** (0.2366 g, 0.38 mmol) in CH$_2$Cl$_2$ (30 mL) and immediately the solution turned bright yellow. After 10 min stirring in the dark the solution was evaporated almost to dryness and *n*-pentane added to the residue, giving **1** as a white solid (0.31 g, 75%).

Method (b). To a yellow solution of [Pt$_2${CH$_2$C$_6$H$_4$P-(C$_6$H$_4$Me-*o*)$_2$}$_2$(S$_2$CNMe$_2$)$_2$Ag{Ag(OClO$_3$)}]ClO$_4$ **5** (0.1525 g, 0.0923 mol) in CH$_2$Cl$_2$ (15 mL) was added PPh$_3$ (0.0484 g, 0.1846 mmol). The mixture was stirred for 20 min and then the solution evaporated almost to dryness. Addition of *n*-pentane to the residue afforded **1** (0.14 g, 70%) (Found: C, 46.44; H, 4.06; N, 1.41. AgC$_{42}$ClH$_{41}$NO$_4$P$_2$PtS$_2$ requires C, 46.35; H, 3.80; N, 1.29%). ($\tilde{v}$/cm^{-1}): 460m, 476s, 488m, 506s, 522s, 563m, 585m, 694vs, 747vs (C^P and PPh$_3$), 958m, 1568vs (Me$_2$NCS$_2^-$), 622s, 1097vs (ClO$_4^-$).

M = Pd (2). *Method (a)*. [Ag(OClO$_3$)(PPh$_3$)] (0.1176 g, 0.2505 mmol) was added to a solution of [Pd{CH$_2$C$_6$H$_4$-P(C$_6$H$_4$Me-*o*)$_2$-*C*,*P*}(S$_2$CNMe$_2$)] **B** (0.1328 g, 0.2505 mmol) in CH$_2$Cl$_2$ (20 mL). The mixture was stirred in the dark for 30 min and then filtered through Celite to remove the small amount of suspended solid. Evaporation of the resulting solution to dryness and addition of Et$_2$O to the residue afforded **2** as a bright yellow solid (0.18 g, 72%).

Method (b). To a yellow solution of [Pd$_2${CH$_2$C$_6$H$_4$P-(C$_6$H$_4$Me-*o*)$_2$}$_2$(S$_2$CNMe$_2$)$_2$Ag{Ag(OClO$_3$)}]ClO$_4$ **6** (0.0761 g, 0.0516 mmol) in CH$_2$Cl$_2$ (25 mL) was added PPh$_3$ (0.027 g, 0.1032 mmol) and the mixture was stirred in the dark for 45 min. Evaporation of the solution almost to dryness and addition of Et$_2$O to the residue yielded **2** (0.0488 g, 47%) (Found: C, 50.70; H, 4.30; N, 1.30. AgC$_{42}$ClH$_{41}$NO$_4$P$_2$PdS$_2$ requires C, 50.47; H, 4.13; N, 1.40%). ($\tilde{v}$/cm^{-1}): 460m, 470s, 480m, 505s, 521s, 560m, 581m, 695vs, 750s (C^P and PPh$_3$), 963m, 1543vs (Me$_2$NCS$_2^-$) 623s, 1091vs (ClO$_4^-$).

[M{CH$_2$C$_6$H$_4$P(C$_6$H$_4$Me-*o*)$_2$-*C*,*P*}(S$_2$CNMe$_2$)Au(PPh$_3$)]ClO$_4$ (M =Pt 3, Pd 4)

M = Pt (3). A solution of [AuCl(PPh$_3$)] (0.1979 g, 0.4 mmol) in CH$_2$Cl$_2$–OEt$_2$ (30:10 mL) was reacted with AgClO$_4$ (0.083 g, 0.4 mmol) for 45 min and the precipitated AgCl was filtered off. The resulting solution containing the [Au(OClO$_3$)(PPh$_3$)] species (0.40 mmol) was treated with [Pt{CH$_2$C$_6$H$_4$P(C$_6$H$_4$Me-*o*)$_2$-*C*,*P*}(S$_2$CNMe$_2$)] (0.247 g, 0.40 mmol) and the solution turned yellow immediately. After 10 min stirring at room

temperature, the solution was evaporated almost to dryness and subsequent addition of OEt$_2$ (20 mL) rendered **3** as a white solid (0.21 g, 44%) (Found: C, 43.62; H, 3.53; N, 1.23. AuC$_{42}$ClH$_{41}$NO$_4$P$_2$PtS$_2$ requires C, 42.85; H, 3.51; N, 1.19%). ($\tilde{\nu}$/cm^{-1}): 464w, 476m, 485w, 510s, 539vs, 563m, 585m, 693vs, 753vs (C^P and PPh$_3$), 1563vs (Me$_2$NCS$_2^-$), 623s, 1100vs (ClO$_4^-$).

M = Pd (4). Compound **4** prepared in a similar manner: [AuCl(PPh$_3$)] (0.1139 g, 0.2302 mmol), AgClO$_4$ (0.0477 g, 0.2302 mmol); [Pd{CH$_2$C$_6$H$_4$P(C$_6$H$_4$Me-*o*)$_2$-*C,P*}(S$_2$CNMe$_2$)] (0.122 g, 0.2302 mmol). Yield: 0.169 g, 67% (Found: C, 45.98; H, 3.62; N, 1.22. AuC$_{42}$ClH$_{41}$NO$_4$P$_2$PdS$_2$ requires C, 46.33; H, 3.80; N, 1.28%). ($\tilde{\nu}$/cm^{-1}): 461w, 469s, 510s, 536s, 559m, 579m, 693s, 753s, 761s (C^P and PPh$_3$), 1532vs (Me$_2$NCS$_2^-$), 623s, 1098vs (ClO$_4^-$).

[Pt$_2${CH$_2$C$_6$H$_4$P(C$_6$H$_4$Me-*o*)$_2$}$_2$(S$_2$CNMe$_2$)$_2$Ag{Ag(OClO$_3$)}}]-ClO$_4$ 5

AgClO$_4$ (0.057 g, 0.275 mmol) was added to a solution of [Pt{CH$_2$C$_6$H$_4$P(C$_6$H$_4$Me-*o*)$_2$-*C,P*}(S$_2$CNMe$_2$)] (0.170 g, 0.275 mmol) in CH$_2$Cl$_2$ (25 mL) and the mixture was stirred for 8 h at room temperature. After filtration of the solid impurities, the solution was evaporated to dryness and *n*-pentane added to the residue giving rise to a solid which was identified as **5** (0.202 g, 89%) (Found: C, 34.84; H, 2.72; N, 1.76. Ag$_2$C$_{48}$Cl$_2$H$_{52}$-N$_2$O$_8$P$_2$Pt$_2$S$_4$ requires C, 34.90; H, 3.17; N, 1.69%) ($\tilde{\nu}$/cm^{-1}): 459m, 475m, 504w, 528w, 562m, 586m, 756s, 770s (C^P), 950w, 1582vs (Me$_2$NCS$_2^-$), 623s, 1095vs (ClO$_4^-$).

Small crystals of **5**·0.5CHCl$_3$·0.125C$_6$H$_{14}$ were grown by slow diffusion of *n*-hexane into a CHCl$_3$ solution of compound **5** at 5 °C.

[Pd$_2${CH$_2$C$_6$H$_4$P(C$_6$H$_4$Me-*o*)$_2$}$_2$(S$_2$CNMe$_2$)$_2$Ag{Ag(OClO$_3$)}}]-ClO$_4$ 6

Equimolar amounts of [Pd{CH$_2$C$_6$H$_4$P(C$_6$H$_4$Me-*o*)$_2$}(S$_2$CN-Me$_2$)] (0.139 g, 0.262 mmol) and AgClO$_4$ (0.0543 g, 0.262 mmol) were dissolved in CH$_2$Cl$_2$–OEt$_2$ (15:7 mL) and reacted for 4 h in the dark. The precipitated solid, **6**, was filtered off (0.1017 g, 53%) (Found: C, 38.39; H, 3.89; N, 1.84. Ag$_2$C$_{48}$Cl$_2$-H$_{52}$N$_2$O$_8$P$_2$Pd$_2$S$_4$ requires C, 39.10; H, 3.55; N, 1.90%). ($\tilde{\nu}$/cm^{-1}): 454m, 470m, 478m, 498w, 517m, 524m, 558m, 583m, 756s (C^P), 947m, 1580vs (Me$_2$NCS$_2^-$), 622s, 1094vs (ClO$_4^-$).

Crystallographic studies

Table 1 reports details of the structure analyses for **1**·1.5CHCl$_3$ and **5**·0.5H$_2$O·0.5CHCl$_3$·0.125C$_6$H$_{14}$. In **1**·1.5CHCl$_3$ two rings of the PPh$_3$ ligand show disorder in some of their carbon atoms over two sets of positions which were refined with 0.5 occupancy. Some restraints in the bond angles and thermal parameters have been applied on one of the CHCl$_3$ solvent molecules. The largest final difference electron density map show two peaks (2.70, 1.08 e Å^{-3}) within 1.1 Å of the heavy atoms.

In **5**·0.5H$_2$O·0.5CHCl$_3$·0.125C$_6$H$_{14}$ all non-hydrogen atoms, except for some belonging to the solvent molecules, were assigned anisotropic displacement parameters. The second silver atom site [Ag(2)/Ag(2′)] is disordered as a result of the coordination of water to one of them Ag(2′) in half of the molecules. The oxygen atoms of one of the ClO$_4$ anions are also disordered over two positions whose occupancies have been refined to 0.53(3) and 0.47(3). Finally, the CHCl$_3$ solvent molecule is also disordered showing two orientations that share two Cl atoms. The occupancy of the non-shared atoms was set to 0.3 and 0.2. The largest final difference electron density features are close to the disordered CHCl$_3$ molecule.

CCDC reference number 186/1166.

References

1 R. Usón and J. Forniés, *Inorg. Chim. Acta*, 1992, **198**, 165 and references therein; R. Usón, J. Forniés, M. Tomás and I. Ara, *Inorg. Chem.*, 1994, **33**, 4023.
2 G. J. Arsenault, C. M. Anderson and R. J. Puddephatt, *Organometallics*, 1988, **7**, 2094.
3 A. F. M. J. van der Ploeg, G. van Koten and K. Vrieze, *Inorg. Chem.*, 1982, **21**, 2026.
4 M. Ebihara, K. Tokoro, K. Imaeda, K. Sakurai, H. Masuda and K. Kawamura, *J. Chem. Soc., Chem. Commun.*, 1992, 1592.
5 M. Ebihara, K. Tokoro, M. Maeda, M. Ogami, K. Imaeda, K. Sakurai, K. Masuda and T. Kawamura, *J. Chem. Soc., Dalton Trans.*, 1994, 3621.
6 A. Albinati, S. Chaloupka, F. Demartin, T. F. Koetzle, H. Rüegger, L. M. Venanzi and M. K. Wolfer, *J. Am. Chem. Soc.*, 1993, **115**, 169.
7 D. Holthenrich, M. Krumm, E. Zangrando, F. Pichierri, L. Randaccio and B. Lippert, *J. Chem. Soc., Dalton Trans.*, 1995, 3275.
8 V. W. W. Yam, P. K. Y. Yeung and K. K. Cheung, *Angew. Chem., Int. Ed. Engl.*, 1996, **35**, 739.
9 (*a*) J. Forniés, A. Martín, R. Navarro, V. Sicilia and P. Villarroya, *Organometallics*, 1996, **15**, 1826; (*b*) L. R. Falvello, J. Forniés, A. Martín, R. Navarro, V. Sicilia and P. Villarroya, *Inorg. Chem.*, 1997, **36**, 6166.
10 M. Nardelli, *Comput. Chem.*, 1983, **7**, 95.
11 R. Usón, J. Forniés, M. Tomás, I. Ara and J. M. Casas, *Inorg. Chem.*, 1989, **28**, 2388.
12 R. Usón, J. Forniés, M. Tomás, J. M. Casas, F. A. Cotton and L. R. Falvello, *Inorg. Chem.*, 1986, **25**, 4519.
13 (*a*) F. A. Cotton, L. R. Falvello, R. Usón, J Forniés, J. M. Tomás, J. M. Casas and I. Ara, *Inorg. Chem.*, 1987, **26**, 1366; (*b*) R. Usón, J. Forniés, M. Tomás, I. Ara, J. M. Casas and A. Martín, *J. Chem. Soc., Dalton Trans.*, 1991, 2253.
14 J. E. Huheey, *Inorganic Chemistry*, *Principles of Structure and Reactivity*, Harper & Row, New York, 3rd edn., 1983.
15 J. Forniés, R. Navarro, M. Tomás and E. P. Urriolabeitia, *Organometallics*, 1993, **12**, 940; J. Forniés, F. Martínez, R. Navarro and E. P. Urriolabeitia, *Organometallics*, 1966, **15**, 1813.
16 D. Coucouvanis, *Prog. Inorg. Chem.*, 1979, **26**, 424.
17 B. J. Hathaway and A. E. Underhill, *J. Chem. Soc.*, 1961, 3091.
18 A. J. Cheney and B. L. Shaw, *J. Chem. Soc., Dalton Trans.*, 1972, 754, 860.
19 G. J. Gainsford and R. Mason, *J. Organomet. Chem.*, 1974, **80**, 395.
20 A. J. Cheney, W. S. McDonald, K. O'Flynn, B. L. Shaw and B. L. Turtle, *J. Chem. Soc., Chem. Commun.*, 1973, 128.
21 A. L. Rheingold and W. C. Fultz, *Organometallics*, 1984, **3**, 1414; W. A. Herrmann, C. Brossmer, K. Öfele, C.-P. Reisinger, T. Priermeier, M. Beller and H. Fischer, *Angew. Chem., Int. Ed. Engl.*, 1995, **34**, 1844.
22 M. Munakata, M. Maekawa, S. Kitagawa, M. Adachi and H. Masuda, *Inorg. Chim. Acta*, 1990, **167**, 181.
23 M. Barrow, H.-B. Buergi, M. Camalli, F. Caruso, E. Fischer, L. M. Venanzi and L. Zambonelli, *Inorg. Chem.*, 1983, **22**, 2356.
24 S. Kitagawa, M. Kondo, S. Kawata, S. Wada, M. Maekawa and M. Munakata, *Inorg. Chem.*, 1995, **34**, 1455.
25 (*a*) G. Smith, A. N. Reddy, K. A. Byriel and C. H. L. Kennard, *Polyhedron*, 1994, **15**, 2425; (*b*) H. Schöllhorn, U. Thewalt and B. Lippert, *Inorg. Chim. Acta*, 1987, **135**, 155.
26 *CRC Handbook of Chemistry and Physics*, Chemical Rubber Publishing Co., Cleveland, 61st edn., 1980, F219.
27 R. Usón, J. Forniés, B. Menjón, F. A. Cotton, L. R. Falvello and M. Tomás, *Inorg. Chem.*, 1985, **24**, 4651.
28 C. E. Housecroft, *Coord. Chem. Rev.*, 1992, **115**, 141.
29 R. Usón and A. Laguna, *Organomet. Synth.*, 1985, **3**, 325.

Paper 8/05099F